

Electromagnetic interrogation of the anisotropic Earth: Looking into the Earth with polarized spectacles

Alan G. Jones*

Dublin Institute for Advanced Studies, 5 Merrion Square, Dublin 2, Ireland

Received 6 October 2005; received in revised form 20 February 2006; accepted 6 March 2006

Abstract

Electrical conductivity of common Earth materials ranges over many orders of magnitude, from $>10^6$ S/m (sulphides, graphite) to $<10^{-6}$ S/m (competent shield rocks). Such a large range of the physical parameter being sensed facilitates high resolution of conducting structures, but an important consequence is that over a large region electromagnetic fields can have vastly different penetration depths from site to site. Thus, adopting interpretation methods used in seismology without appropriate adaptation is inappropriate. In particular, geoelectrically determined strike arrows at a given period should not be portrayed as equivalent to maps of SKS arrows with the same inherent depth information. In addition, there are structures for which depth penetration is radically different for the two modes of propagation (TE and TM) in 2D structures. An extreme example, but encountered in the real Earth, is a class of structures with significant responses in the MT mode with electric field parallel to structures (TE mode) to the presence of anomalous conductivity, but for which the responses in the mode with the electric field perpendicular to structures (TM mode) are negligible. In this case, the upper anisotropic layer acts as a polarizing filter, and only TM mode fields penetrate through it. Thus no tensor information is available for the lower layers, and variation in structural strike directions with increasing depth is irresolvable. © 2006 Elsevier B.V. All rights reserved.

Keywords: Electromagnetic induction; Magnetotellurics; Tensor decomposition; Electromagnetic modelling; Anisotropy

1. Introduction

There are two means of interrogating the Earth directly for its current in situ physical properties, namely observing the transmission of either seismic or electromagnetic waves. Whereas seismic methods commonly give bulk property information of the rock matrix, i.e., compressional and shear velocities, electromagnetic induction methods inherently sense the presence of a partially interconnected conducting phase, yielding bulk electrical conductivity (e.g., Everett, 2005). In the vast

majority of cases, the two together provide enhanced constraints not afforded by either alone (examples discussed in Jones, 1998, 1999). As a caution though, one must be assured that the surface seismological and electromagnetic observations are phenomenologically related and can be validly interpreted as resulting from the same behaviour of the Earth, and not due to a problem of resolution from surface observations (see e.g., Cook and Jones, 1995).

Seismological methods have provided by far most of the physical property information about the Earth's lithosphere. Recently though, with the advent of high-quality, low-frequency magnetometers (e.g., Narod and Bennest, 1990), electromagnetic (EM) surveys, using the natural-source magnetotelluric (MT) method, have

* Tel.: +353 1 662 1333; fax: +353 1 662 1477.
E-mail address: alan@cp.dias.ie.

been contributing to knowledge of lithospheric geometries (e.g., Jones, 1999), and thereby aiding in advancing theories about formation and evolution processes. One prime example is the Archean Slave craton in northwestern Canada. Seismological teleseismic investigations determined the detailed seismic stratigraphy beneath the southeastern part of the craton (Bostock and Cassidy, 1997; Bostock, 1998), and regional-scale lateral variation across the craton (Bank et al., 2000; Snyder et al., 2003, 2004). MT surveys across the Slave craton also yielded craton-scale variation in the sub-continental lithospheric mantle (SCLM), with the serendipitous discovery of an upper mantle conductor beneath the central part of the craton, named the Central Slave Mantle Conductor (Jones et al., 2001a,b, 2003). The seismic and EM results, taken together with geological and geochemical observations, suggest a tectonic history for the Slave's SCLM that post-dates initial formation (Davis et al., 2003).

Over the last decade, observations of shear wave splitting from subvertical rays passing through the Earth's core (the SKS and SKKS phases) have predominantly been interpreted either in terms of fossilized strain-induced fabric (Silver and Chan, 1988, 1991; Silver, 1996), or in terms of basal drag of the lower lithosphere from present-day plate movements (Vinnik et al., 1984, 1992). For both of these interpretations, the determined SKS delay times have a ready explanation, given the intrinsic seismic velocity anisotropy of olivine as observed in the laboratory, in terms of preferentially aligned olivine crystals; although the interpretations sometimes test the bounds of credulity by assuming that continental mantle lithosphere is ordered at a very high level. However, the SKS method does suffer from an intrinsic lack of depth resolution; the anisotropy can occur anywhere on the path of the teleseismic arrival from the core–mantle boundary to the surface.

The existence of electrical anisotropy, especially in crustal rocks, rather than heterogeneity is becoming more appreciated by the EM community, and an excellent recent review by Wannamaker (2005) describes the phenomenon and some field observations. Deep-probing EM studies began to report observations of electrical anisotropy in the deep crust and upper lithospheric mantle in the eastern part of the Superior Province in early-1990s (Kellett et al., 1992; Kurtz et al., 1993; Mareschal et al., 1995). The anisotropy detected is of two orders of magnitude, rather than a few percent as in the seismic case. Such large mantle anisotropy cannot be explained in terms of intrinsic crystal or grain electrical anisotropy: dry olivine at lithospheric conditions displays comparatively little electrical anisotropy in the

laboratory (anisotropy factor of <2.5 , Du Frane et al., 2005). It is only when hydrogen diffusion is considered that large anisotropies may result, because diffusion on the $[1, 0, 0]$ axis is 20 times greater than on the $[0, 1, 0]$ axis, and 40 times greater than on the $[0, 0, 1]$ axis (Kohlstedt and Mackwell, 1998). However, numerical studies by Simpson and Tommasi (2005), with random resistor networks, suggest that in the real Earth diffusion will account for an anisotropy factor of 3 at best. Everett (2005) though does raise a valid point about the applicability of such network approaches, initiated with Madden (1976, 1983) and more recently advocated by Bahr (1997), Bahr et al. (2002) and Bigalke (1999, 2003), for simulating EM induction in rocks.

The observed obliquity between seismic SKS fast directions and the electrical most conductive directions for collocated sites in the eastern Superior Province was interpreted by Ji et al. (1996) in terms of an Archean shear sense indicator. Tommasi et al. (1999) discuss this proposal, and conclude that obliquity should not be observed in regions that have experienced very low or high shear strains. In the former case, both directions should be oblique to the shear zone, and in the latter both should be parallel to the shear zone. Confirmation of this latter high strain case came recently from Eaton et al. (2004), who compared the results from teleseismic (Eaton and Hope, 2003) and MT (Wu et al., 2002) experiments across the Great Slave Lake shear zone in northern Canada, and showed that the MT and SKS directions for mantle lithospheric depths were within error of each other. Padilha et al. (2005) also observe parallel SKS and electrical strike directions. In stark contrast, Hamilton et al. (2006) present evidence that SKS observations on the Kaapvaal craton are not parallel, and in fact are almost exactly 90° different, with observations of the most conductive direction within the mantle cratonic lithosphere.

Given the apparent success with which SKS observations have been interpreted in terms of tectonic processes, and the possible link between seismic and electrical anisotropy directions, there has been an enthusiasm by some within the EM community for portraying geoelectric strike information, gleaned primarily from the phase difference in two orthogonal directions, at a given frequency as also qualitatively interpretable in terms of tectonics (e.g., Boerner et al., 2000; Simpson, 2001, 2002; Bahr and Simpson, 2002; Gatzemeier and Moorkamp, 2005). The purpose of this paper is to emphasize that such an approach is potentially fraught with difficulty, and may, in circumstances not that unusual, lead to inappropriate inferences. This caution has been expressed by Jones et al. (2005a,b) for two regions of Canada, whereas herein the problem is

shown for three regions known to exhibit high crustal anisotropy.

The problem for estimating electrical anisotropy, especially its variation with depth, is due to the vast range of the parameter that EM measurements are primarily sensitive to, namely electrical conductivity. Seismic velocities vary laterally by less than 10%, so that when one considers the propagation characteristics of Love and Rayleigh surface waves in different directions at various frequencies (e.g., [Debayle and Kennett, 2000a,b](#)), one can be assured that they are representative of approximately the same depth ranges. In contrast, electrical conductivity varies by many orders of magnitude, which raises two problems: there can be significant variations in the depth of penetration between sites in a large-scale regional survey, and at a single site there can be a significant difference in the depth of penetration in orthogonal directions.

Estimates for the Superior craton suggest two orders of magnitude difference between the most conducting and least conducting directions ([Mareschal et al., 1995](#)). These anisotropy estimates come from full 2D modelling of the responses, not merely from consideration of the magnitude of the observed phase differences. EM wave propagation is more attenuated when the electric field is parallel to the conducting direction (typically the so-called transverse electric, TE, mode of propagation, also called E-polarization or E-parallel), than when it is oriented perpendicular to it (the transverse magnetic, TM, mode of propagation, also called B-polarization, H-polarization, or E-perpendicular). The consequence is that the conducting (TE) mode requires longer periods to penetrate to the same depths as does the resistive (TM) mode. [Ferguson and Edwards \(1994\)](#) previously highlighted that the two modes sense different depth ranges in the presence of surface conductors.

Below I present three cases that illustrate that one must interpret geoelectric strike directions at a particular period with care. The first case presents an extreme, but not uncommon, example, which is a class of Earth structures with a significant TE response, but for which the TM response is negligible. Geologically, these are often en-echelon, sub-vertical conducting structures that have been observed in a number of regions, including the North American Central Plains anomaly within the Paleoproterozoic Trans-Hudson Orogen. In such cases, the TE mode signals are almost completely attenuated within the crust, even to very long periods, whereas the TM mode data at the same periods are sensitive to electric conductivity to deep within the lithosphere (100+ km). Thus, the crust acts as a polarizing filter, only permitting penetration by the TM mode EM waves and

arresting penetration by TE mode waves. An important consequence for the mantle is that one can only obtain information in the direction that is the crustal TM direction, which may not accord with mantle strike at all; one cannot obtain any tensor information.

The second example is when the crust and mantle have known different geoelectric and SKS directions, and comes from the Great Slave Lake shear zone in northern Canada. As the anisotropy is not strong within the crust (less than an order of magnitude), it is possible to obtain the correct lithospheric mantle geoelectric strike direction. However, if the anisotropy were stronger then it would be impossible to obtain the lithospheric mantle geoelectric strike direction, and erroneous conclusions would be drawn.

The third case is an examination of the expected result for central Australia, based on the results of [Debayle and Kennett \(2000a\)](#). Given the expected high electrical anisotropy inferred from the observed high seismic anisotropy, MT data within the 1000–10,000 s band of periods result from very different depth penetration.

These problems, of comparing data with different depth penetration, require some form of first-order depth normalization prior to interpretation. Recent examples of such an approach are from [Jones et al. \(2005a,b\)](#), who convert the MT data from period to depth prior to deriving and mapping anisotropy coefficients, and [Hamilton et al. \(2006\)](#) and [Padilha et al. \(2006\)](#), who derive the depth penetration along a profile and plot anisotropy information within given depth ranges.

2. North American central plains anomaly: strong single-layer anisotropy

The North American central plains (NACP) conductivity anomaly, in central North America, is possibly the longest crustal conductivity anomaly on Earth. It has been mapped over a distance of >3000 km, from southern South Dakota to western Hudson Bay ([Jones and Craven, 1990](#); [Jones et al., 2005b](#), and references therein), and possibly extends across Greenland to Scandinavia ([Jones, 1993a](#)). It has been shown to lie wholly within the Paleoproterozoic Trans Hudson Orogen, the orogen that closed the >5000 km-wide Manikewan ocean ([Stauffer, 1984](#)) and welded together the Superior Province to the east with the Wyoming/Churchill (Rae-Hearne) Provinces to the west ([Hoffman, 1988](#)). For much of its length, particularly beneath the Williston Basin in southern Saskatchewan and North Dakota, the NACP has an unusual response: it has a very strong TE response but virtually no TM response ([Jones, 1993b](#); [Jones et al., 1993, 2005b](#)). The conductive bodies have an

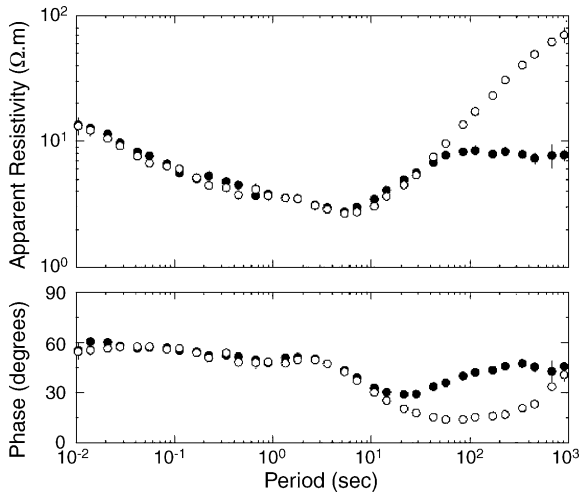


Fig. 1. Observed MT data at a site on top of the NACP anomaly (site PC5014 of Jones et al., 1993). The along-strike data (TE mode) are shown as full circles, and the across-strike data (TM mode) as open circles.

along-strike resistivity of the order of 1–3 Ω m, and an across-strike resistivity of >300 Ω m. Laboratory studies on rock samples from exposures of the anomaly showed greater than two orders of magnitude in electrical anisotropy at the hand-sample scale (Jones et al., 1997), and that this could be attributed to sulphides that migrated to fold hinges during orogenic compression, with pyrite grains connected along strike but disconnected across strike. The MT data from a site on top of the NACP are shown in Fig. 1 (site PC5014 of Jones, 1993b).

Fig. 2A shows a model of the NACP anomaly developed by Jones and Craven (1990). It is representative of the suite of acceptable models derived from the MT data recorded along a profile in southern Saskatchewan (Jones, 1993b). The isotropic conductive blocks cannot be connected, or a TM response would be generated that is not observed (Jones, 1993b).

Another way of representing the anomalous region is as an anisotropic body. Fig. 2B shows a schematic representation of such a body, and its forward response was calculated using the 2D anisotropy code of Pek and

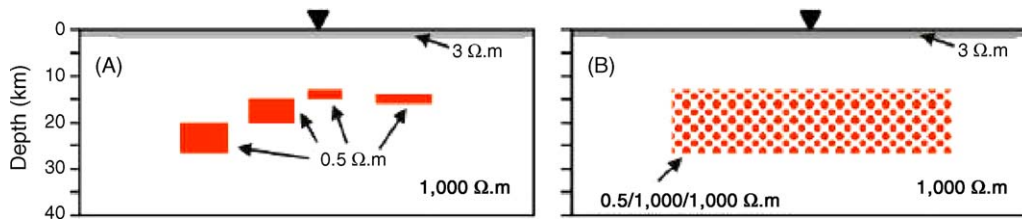


Fig. 2. Two 2D models of the NACP crustal anomaly. (A) Model presented by Jones and Craven (1990) of separate conducting blocks of resistivity of 0.5 Ω m. (B) Model that yields the same responses with an anisotropic region (boxed) with an along strike (ρ_x) resistivity of 0.5 Ω m, and an across strike resistivity (both laterally and vertically, ρ_x and ρ_z) of 1000 Ω m.

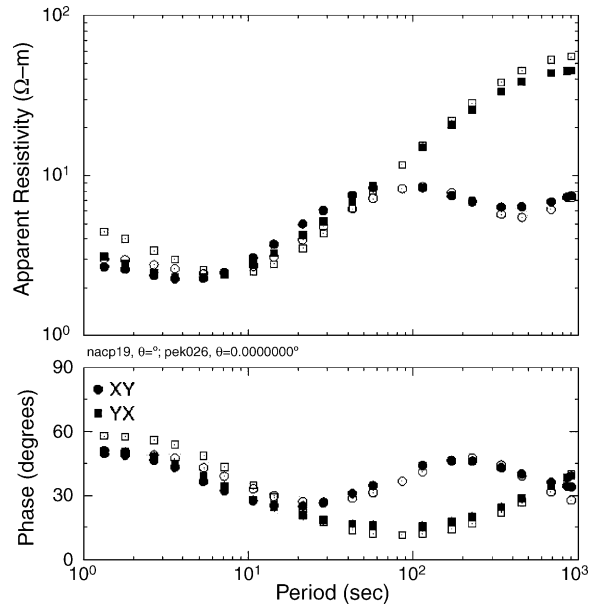


Fig. 3. Comparison of observed data (open symbols—TE: circles; TM: squares) with the theoretical response from the anisotropic model shown in Fig. 2B (full symbols—TE: circles; TM: squares).

Verner (1997). The anomalous body has an along strike (ρ_x) resistivity of 0.5 Ω m, and an across strike resistivity (both laterally and vertically, ρ_y and ρ_z) of 1000 Ω m. The lithosphere is modelled as 100 km thick, with a basal conducting layer below of 10 Ω m. The forward responses observed at the centre site for these two models (Fig. 2A and B) are shown in Fig. 3, together with the observations from the central site (Fig. 1).

One consequence of the existence and nature of the NACP conductor is that the TE EM fields are strongly attenuated by the conductor, whereas the TM fields are not. This is shown by EM attenuation with depth for 1D models with and without the conductor, representing the TE and TM modes, respectively. The E- and H-field attenuation at a period of 300 s for the 1D model with the conductor is shown in Fig. 4. In this model, the Phanerozoic sediments are represented by a 2 km thick layer of 2.5 Ω m, below which is a crustal and upper mantle layer

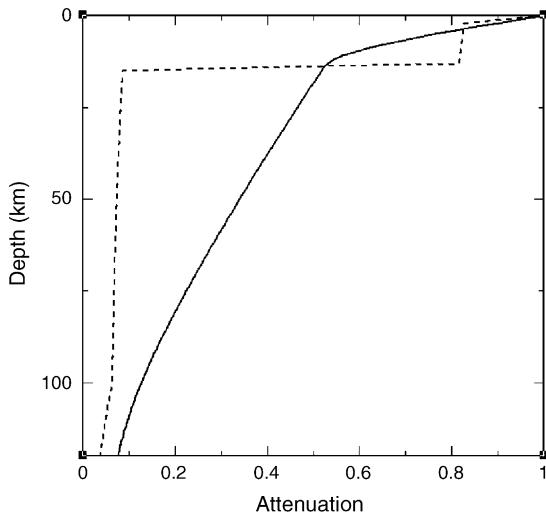


Fig. 4. 1D electromagnetic field attenuation with depth at a period of 300 s for a site on top of the NACP conductor. Solid line: electric field attenuation. Dashed line: magnetic field attenuation. The model comprises a top layer, representing the Phanerozoic sediments, of 2 km thickness and 2.5 Ω m, below which is a crustal and upper mantle layer of 200 Ω m underlain by an asthenosphere of 10 Ω m at a depth of 100 km. Within the crust is an anomalous conducting layer between 13 and 15 km of 0.5 Ω m representing the NACP conductor.

of 200 Ω m underlain by an asthenosphere of 10 Ω m at a depth of 100 km. Within the crust is an anomalous conducting layer between 13 and 15 km of 0.5 Ω m (total conductance of 4000 S) representing the NACP conductor. Note the severe magnetic field attenuation as soon as the conductor is sensed.

The total EM amplitude is calculated from the square root of the energy in the Poynting vector, given by E-field amplitude times the H-field amplitude at the same depth. In a half-space these two would be the same, but in a layered Earth they are very different due to the physical differences in penetration (see e.g., Jones, 1983a).

It should be appreciated that using the EM field amplitude as a representation of sensitivity to structure is only approximate. The formal sensitivity is given by the Frechet derivative of the off-diagonal components of the impedance tensor, which, for the 1D isotropic layered Earth case, has been shown to be proportional to the square of the electric field at depth normalized by the surface electric field, i.e. $(E_x(z)/E_x(0))^2$ (e.g., Oldenburg, 1979; Gómez-Trevino, 1987) for the Z_{xy} component. However, this electric field expression belies the fact that sensitivity must also be a function of the magnetic field at depth, $H_y(z)$; if the magnetic field is vanishingly small, then there will be no electric field induced. Given the 1D relationship $E_x(z) = Z_{xy}(z)H_y(z)$, then we can recast the Frechet derivative in terms of $(E_x(z)H_y(z)/(E_x(0)H_y(0)))$, scaled by the ratio of the

impedance at depth divided by the surface impedance. This EM field term is the energy of the normalized Poynting vector, whereas I use its amplitude. For non-1D isotropic layered Earth cases, such as 1D with anisotropic layers, 2D, 2D with 3D distortion, or full 3D, then the Frechet derivative is far more complex (see e.g., Pek and Santos, 2002, for the anisotropic 1D case), but whatever the complexity, the attenuation of the EM fields will be indicative of sensitivity.

EM attenuation for the two 1D models, which represent the two 2D modes, over a range of periods is contoured in Fig. 5, where Fig. 5A represents the TE mode and Fig. 5B represents the TM mode. The black line represents the $1/e$ (0.37) amplitude level, i.e., equivalent to the skin depth for a uniform half space. The attenuation of the EM fields within the 13–15 km depth range, where the anomaly lies, is apparent in Fig. 5A. At the base of the crust (40 km) EM fields have an amplitude of $1/e$ of the surface value at a period of 200 s for TM mode propagation (Fig. 5B), but at a much longer period of 1000 s for TE mode propagation (Fig. 5A). Indeed, the TE field amplitude is not greater than $1/3$ below the body until periods >850 s have been reached. At longer periods the TE field attenuation gradient is less than that for the TM fields, such that TE field penetration increases rapidly with period to approach that of the TM field (compare the solid lines on Fig. 5), but even for the longest realistic periods (100,000 s) the two do not have the same depth penetration.

One interesting effect is also apparent in Fig. 5. Attenuation of EM fields depends in part on the conductivity structure below the depth of interest, as well as that overlying it. This can be seen by the period at which the skin depth attenuation exceeds the thickness of the Phanerozoic sediments. For the model without the NACP conductor, this period is approx. 30 s (black line on Fig. 5B). In contrast, for the model with the conductor, this period is slightly greater than 10 s (black line on Fig. 5A).

To compensate to first order for this phenomenon of varying penetration depths with differing polarization, the apparent resistivity and phase data can be transformed from period to approximate depth using the Niblett–Bostick transformation (Niblett and Sayn-Wittgenstein, 1960; Bostick, 1977; Jones, 1983b). The formula for the depth, h , is:

$$h \text{ (m)} = \sqrt{\frac{\rho_a(T)T}{2\pi\mu_0}}.$$

Note that this penetration depth is for an attenuation factor of approximately $1/2$ instead of the more usual skin depth attenuation of $1/e$.

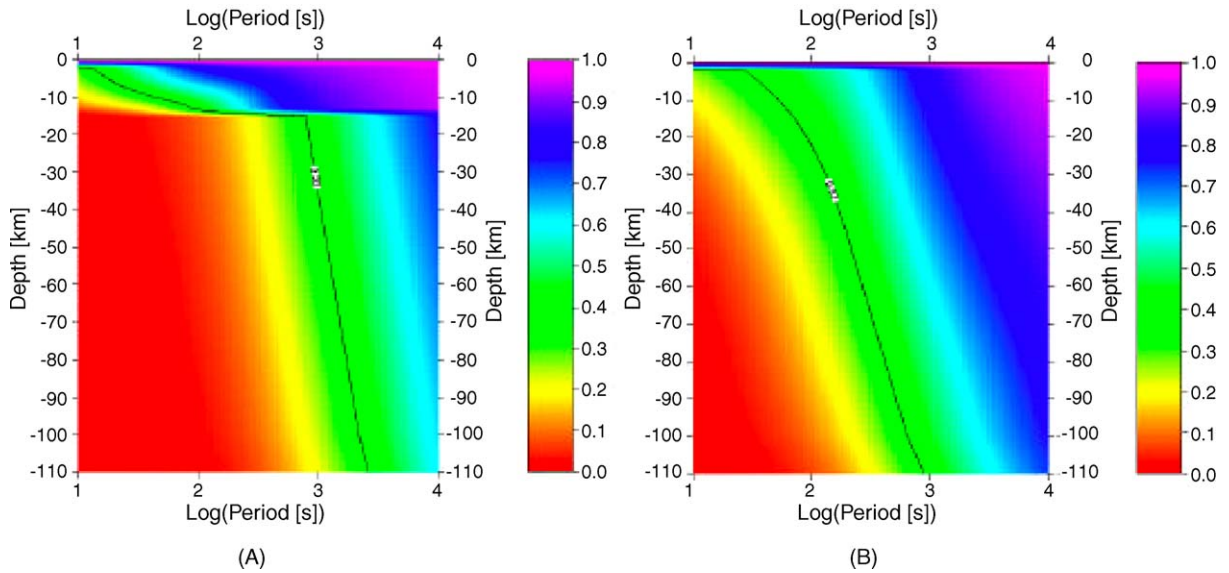


Fig. 5. EM attenuation, with period and depth, for the two 1D models at the site above the NACP. (A) Attenuation for model with conductor, i.e., equivalent to 2D TE mode data. (B) Attenuation for model without conductor, i.e., equivalent to 2D TM mode data. The black line represents the $1/e$ amplitude level, i.e., equivalent to the skin depth for a uniform half space.

For the data from above the NACP anomaly, when transformed into the approximate depth domain the responses more correctly display penetration depth (Fig. 6). Even the longest period TE mode data (1000 s) are not sensing below the crust. Clearly, for such a situation when determining anisotropy the 1000 s TE responses, which penetrate to ~ 30 km, should be com-

pared with the 200 s TM responses, not with the 1000 s TM responses. Of particular concern is that there is no tensor information possible for the mantle: the only information is in the crustal TM mode direction, which may or may not be the TM mode in the mantle.

It must be appreciated that this approach is a first-order approximation of the true physics. The Niblett–Bostick transformation from period to depth is not a rigorous depth conversion, and is only formally applicable in 1D situations or situations where the responses act as 1D. In this case, the effect of the NACP conductor is so strong in one 2D mode (TE mode), and not the other, that the two modes can be treated as two independent 1D models. In general situations this may not hold, however applying the transformation and considering the MT parameters in approximate depth is far superior to merely comparing responses in the two orthogonal directions at the same frequency.

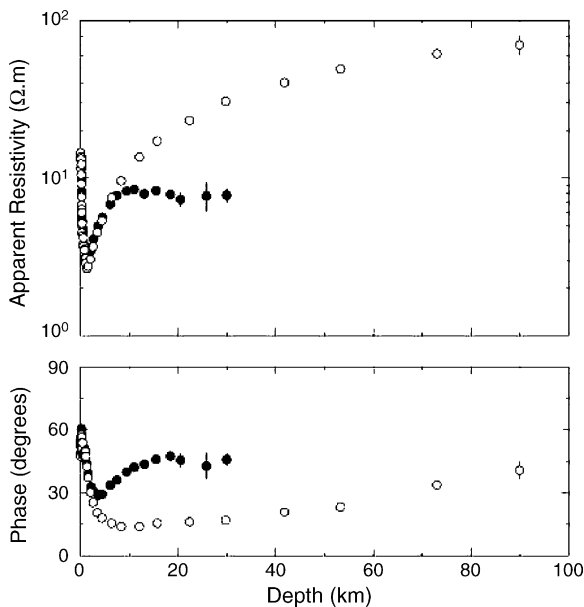


Fig. 6. MT data of Fig. 1 represented in terms of approximate depth rather than period, using the Niblett–Bostick depth transformation.

3. Great Slave Lake shear zone: weak two-layer anisotropy

The Great Slave Lake shear zone (GSLsz) has been studied both electrically and seismically in two consecutive geophysical experiments. Wu et al. (2002) provide an electrical resistivity model of the region from MT data acquired as part of the Lithoprobe SNORCLE transect investigations (Cook and Erdmer, 2005), whereas Eaton and Hope (2003) provide an SKS analysis of teleseismic observations along the same profile (but not at collocated

sites). Eaton et al. (2004) demonstrate that both respond to two-layer anisotropy.

The crust (to approx. 40 km) shows an electrical strike of $\sim N30^\circ E$, and a lithospheric mantle strike of $\sim N60^\circ E$ (see Wu et al., 2002; Eaton et al., 2004). Seismically, the sites within the shear zone exhibit an upper layer strike of $\sim N20^\circ E$, and a lower layer of $\sim N66^\circ E$ (see Eaton and Hope, 2003; Eaton et al., 2004). Taken together, the clear inference is that the crust and mantle are decoupled and have different intrinsic strike directions, and that the electrical and seismic strikes are parallel, to within error. Thus, one important conclusion from this work is that the inherent depth ambiguity in SKS observations can be addressed through collocated MT measurements.

In order to determine the representative effect (not to model the actual responses observed), the forward responses of a 1D four-layer Earth containing two anisotropic layers with parameters of:

- layer 1 (upper crust): $\rho_x = \rho_y = \rho_z = 10,000 \Omega \text{ m}$, $h = 10 \text{ km}$;
- layer 2 (lower crust): $\rho_{30} = \rho_z = 100 \Omega \text{ m}$, $\rho_{120} = 1000 \Omega \text{ m}$, $h = 30 \text{ km}$;

- layer 3 (mantle lithosphere): $\rho_{60} = \rho_z = 30 \Omega \text{ m}$, $\rho_{150} = 1000 \Omega \text{ m}$, $h = 160 \text{ km}$;
- layer 4 (asthenosphere): $\rho_x = \rho_y = \rho_z = 30 \Omega \text{ m}$, half space;

where h denotes layer thickness, ρ_x , ρ_y and ρ_z denote the north, east and vertical resistivity, respectively, and ρ_{nn} denotes the resistivity in a horizontal direction NN degrees clockwise from north (i.e., $\rho_x = \rho_0$, and $\rho_y = \rho_{90}$), were derived using the approach and code of Pek and Santos (2002). The parameters were taken from the 2D resistivity model of Wu et al. (2002) as representative of the electrical structure in the vicinity of the GSLsz. Note that anisotropic mantle lithosphere abuts directly against anisotropic lower crust. Geoelectric strike was determined from these responses, using the Groom and Bailey (1989) tensor decomposition approach extended by McNeice and Jones (2001), and the derived strike directions, with an averaging frequency window of 1/3 of a decade, are shown in Fig. 7B.

These synthetic strikes are to be compared with those observed experimentally. Fig. 7A shows the strike directions observed for the sites across the GSLsz, and there

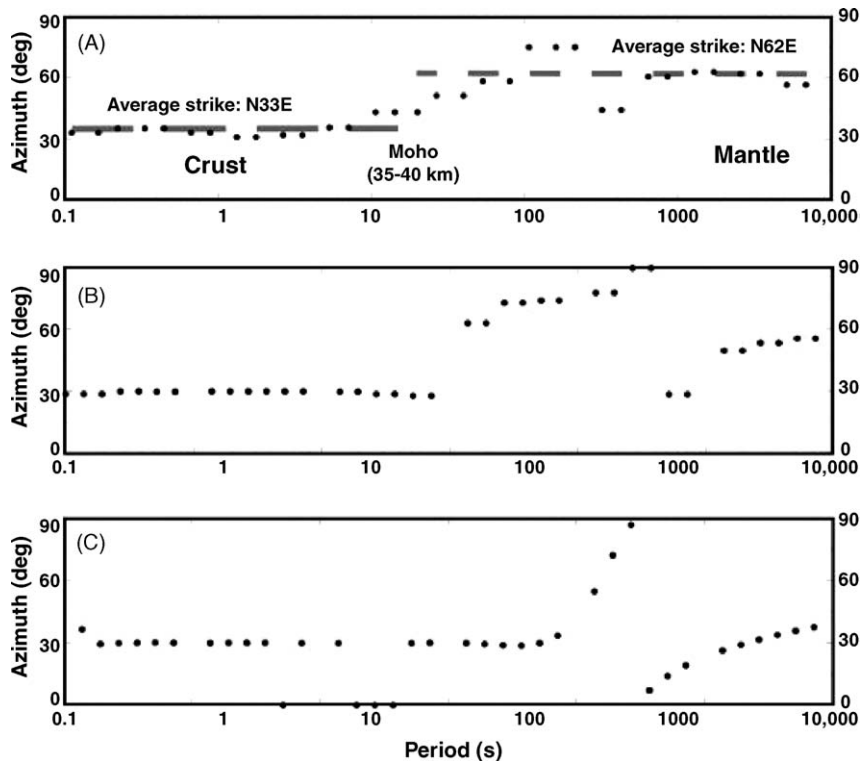


Fig. 7. (A) Strike directions observed for sites across the Great Slave Lake shear zone (from Wu et al., 2002). (B) Theoretical strike directions for a four-layer model with two anisotropic layers for the shear zone. (C) Theoretical strike directions for a four-layer model with two anisotropic layers but with enhanced crustal anisotropy (factor of 10 greater than (B)).

is good comparison between the observed strikes and the ones computed from the above model.

The question arises about how effectively these strike determination methods operate in the presence of larger upper layer anisotropy, such as observed for the NACP. To replicate this effect the forward responses were derived for the model above, except with a lower crustal layer of $\rho_{30} = \rho_z = 10 \Omega \text{ m}$, i.e., two orders of magnitude anisotropy not one as observed. The strike determinations are shown in Fig. 7C, and it is clear that even at the longest periods used (10,000 s), the actual anisotropy direction of the lithospheric mantle cannot be determined. Indeed, taking the data from the longest period decade, of 1000–10,000 s, one obtains a best-fit strike direction to all of the data of 32° , i.e., the crustal strike direction.

4. Australasia: strong two-layer anisotropy

The results of Debayle and Kennett (2000a,b) for central Australia are remarkable in that they demonstrate unequivocal evidence for two-layer azimuthal anisotropy in SV within the lithosphere, and with virtually a 90° change in orientation of the fast propagation direction and up to 9% variation in wavespeed in orthogonal directions. These observations agree qualitatively with those of Simons and van der Hilst (2003). The upper layer in central Australia, above 150 km, has a fast polarization direction of approximately east–west, and is concluded to be a fossilized anisotropy formed at creation, whereas the lower layer, to approx. 250 km, has a north–south fast polarization direction, and is concluded to be a consequence of modern plate movement (Debayle and Kennett, 2000b). Intriguingly, and beyond the scope of this paper, there is significant complexity in SKS determinations at the same stations (Heintz and Kennett, 2005), from which one does not draw the same conclusions as for the surface wave studies.

Assuming that the crust is isotropic, and that the large scale of anisotropy observed seismically translates into a correspondingly large change in electrical anisotropy, a possible equivalent electrical model for central Australia is:

- layer 1 (crust): $\rho_x = \rho_y = \rho_z = 10,000 \Omega \text{ m}$, $h = 40 \text{ km}$;
- layer 2 (upper mantle lith.): $\rho_{90} = \rho_z = 30 \Omega \text{ m}$, $\rho_0 = 1000 \Omega \text{ m}$, $h = 110 \text{ km}$;
- layer 3 (lower mantle lith.): $\rho_0 = \rho_z = 30 \Omega \text{ m}$, $\rho_{90} = 1000 \Omega \text{ m}$, $h = 100 \text{ km}$;
- layer 4 (asthenosphere): $\rho_x = \rho_y = \rho_z = 30 \Omega \text{ m}$, half space.

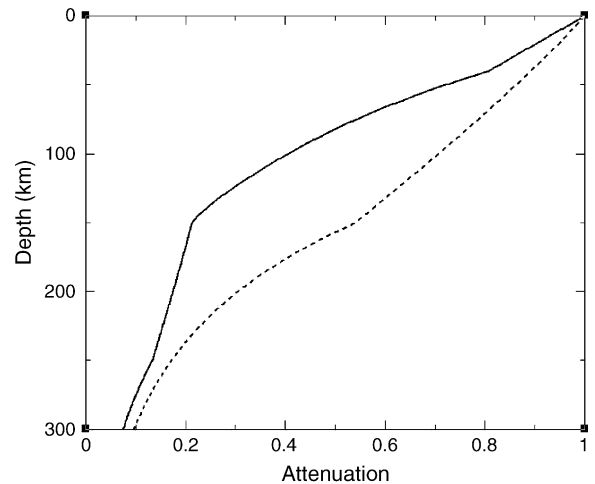


Fig. 8. EM attenuation at 1000 s for a site in the centre of Australia based on an expected theoretical Anisotropic model. Solid line: attenuation for EW currents. Dashed line: attenuation for NS currents.

Because of the nature of the anisotropy, in that the two anisotropic layers are orthogonal to each other, the responses observed on the surface are those of two independent 1D models, with a three-layer model for N–S currents of 10,000/1000/30 $\Omega \text{ m}$ with interfaces at 40 and 150 km, and a four-layer model for E–W currents of 10,000/30/1000/30 $\Omega \text{ m}$ with interfaces at 40, 150 and 250 km.

For these two models, the penetration depths (given by the depth at which the EM field amplitude is 0.37 of the surface value) at a period of 1000 are 185 and 105 km for the N–S and E–W models, respectively. EM attenuation with depth for the two models at 1000 s period shows the different penetration, with the E–W currents (Fig. 8, solid line) much more strongly attenuated in the upper mantle lithosphere, and the N–S currents (Fig. 8, dashed line) more strongly attenuated in the lower lithosphere. However, the two virtually coalesce at the base of the lithosphere (250 km) as both the TE and TM data have, by then, passed through almost the same total depth-integrated conductance. At 10,000 s the penetration depths are virtually the same, namely 355 and 350 km. Thus, in the period band studied by Simpson (2001), of 1000–10,000 s, the MT data from the orthogonal observations are, most likely, sensitive to very different depths.

5. Discussion and conclusions

Determining the anisotropy of the lithosphere potentially holds the key to understanding its formation and deformation processes. Observations of seismic anisotropy, led by SKS analyses but increasingly of

surface wave anisotropy, have made significant contributions to those debates. Similarly, observations of electrical anisotropy, initiated with the seminal contribution by Mareschal et al. (1995), are attempting to provide further constraints. However, caution must be exercised with electrical anisotropy studies due to the vast range possible for electrical conductivity resulting in greatly differing penetration depths at different sites, and between the two modes at the same sites.

Hamilton et al. (2006) demonstrate that EM fields at sites acquired along the same profile have vastly different penetration depths for the same periods. Sites on conductive crustal features are only penetrating 20 km at periods of 1000 s or greater, whereas on highly resistive regions this depth penetration is reached by 1 s. They compensate for this by determining the depth penetration at each site, and portraying the strike arrows in terms of depth bands.

For the NACP anomaly there is significantly different depth penetration for the two orthogonal modes of penetration in the crust. The same situation exists for MT data acquired in Alberta by Boerner et al. (1999, 2000). The TE data do not sense below the crust, i.e., the long period TE data only have a depth penetration of crustal dimensions, due to the presence of highly anisotropic crustal structures, whereas the TM data pass through the crust virtually without attenuation. Thus, the only information that can be obtained about the mantle is in a single direction that is the crustal TM mode direction; there is no tensor information possible at mantle depths. The problem is that whereas one is assured of mode identification within the crust, below the crust there is only information from a single direction, which is the TM direction in the crust, and thus there is no knowledge of structural or intrinsic anisotropy. Thus on modelling of the data Boerner et al. (1999) had to make the assumption that the TM mode in the crust is valid in the lithospheric mantle, and model the MT data accordingly. As shown for quite a number of studies, such as the Great Slave Lake shear zone (above) and the study across the Snowbird Tectonic Zone (Jones et al., 2002), the crust and mantle are often decoupled, so assumptions about vertical continuity of geoelectric strike direction are highly questionable.

Clearly, maps of geoelectric strike at even the longest periods can be misleading because of crustal effects. This argument was raised by Korja et al. (2002, 2003) and Lahti et al. (2005), who demonstrated that crustal effects observed in Fennoscandia can account for observed strike directions at even very long periods, and thus dispute the conclusions of Bahr and Simpson (2002) based on geoelectric strikes observed at 2049 s. In their

work, Hamilton et al. (2006) and Padilha et al. (2006) compensate for this problem by converting the data to approximate depth, and presenting maps for varying depths rather than varying periods. However, compensation must be undertaken for the two modes, as well as between sites.

It should be appreciated that these concerns extend also to galvanic tensor decomposition approaches to determine the dominant 2D strike direction, and to extract the 2D regional impedances (e.g., Zhang et al., 1987; Bahr, 1988; Groom and Bailey, 1989; Chakridi et al., 1992; Chave and Smith, 1994; Smith, 1995, 1997; Chave and Jones, 1997; McNeice and Jones, 2001). Clearly if geoelectric strike varies with depth, then there is the potential for mixing modes when there is strong anisotropy, and erroneous conclusions will result.

Acknowledgements

Josef Pek is thanked for providing his 1D and 2D anisotropic forward codes (Pek and Verner, 1997; Pek and Santos, 2002). Dublin Institute for Advanced Studies publication number GPxxx. Substantial reviews from Ian Ferguson, John Weaver, and Acting Editor Dave Eaton significantly improved this paper.

References

- Bahr, K., 1988. Interpretation of the magnetotelluric impedance tensor: regional induction and local telluric distortion. *J. Geophys.* 62, 119–127.
- Bahr, K., 1997. Electrical anisotropy and conductivity distribution functions of fractal random networks and of the crust: the scale effect of connectivity. *Geophys. J. Int.* 130, 649–660.
- Bahr, K., Simpson, F., 2002. Electrical anisotropy below slow- and fast-moving plates: paleoflow in the upper mantle? *Science* 295, 1270–1272.
- Bahr, K., Smirnov, M., Steveling, E., 2002. A gelation analogy of crustal formation derived from fractal conductive structures. *J. Geophys. Res.* 107, doi:10.1029/2001JB000506.
- Bank, C.-G., Bostock, M.G., Ellis, R.M., Cassidy, J.F., 2000. A reconnaissance teleseismic study of the upper mantle and transition zone beneath the Archean Slave craton in NW Canada. *Tectonophysics* 319, 151–166.
- Bigalke, J., 1999. Investigation of the conductivity of random networks. *Phys. Stat. Mech. Appl.* 272, 281–293.
- Bigalke, J., 2003. Analysis of conductivity of random media using dc, MT, and TEM. *Geophysics* 68, 506–515.
- Boerner, D.E., Kurtz, R.D., Craven, J.A., Ross, G.M., Jones, F.W., Davis, W.J., 1999. Electrical conductivity in the Precambrian lithosphere of Western Canada. *Science* 283, 668–670.
- Boerner, D.E., Kurtz, R.D., Craven, J.A., Ross, G.M., Jones, F.W., 2000. A synthesis of electromagnetic studies in the Lithoprobe Alberta Basement Transect: constraints on Paleoproterozoic indentation tectonics. *Can. J. Earth Sci.* 37, 1509–1534.

- Bostick, F.X., 1977. A simple almost exact method of MT analysis. In: Workshop on Electrical Methods in Geothermal, Exploration, U.S.G.S., Contract, No. 14080001-8-359, Reprinted in Vozoff (1986).
- Bostock, M.G., 1998. Mantle stratigraphy and evolution of the Slave province. *J. Geophys. Res.* 103, 21, 183–21, 200.
- Bostock, M.G., Cassidy, J.F., 1997. Upper mantle stratigraphy beneath the southern Slave Craton. *Can. J. Earth Sci.* 34, 577–587.
- Chakridi, R., Chouteau, M., Mareschal, M., 1992. A simple technique for analysing and partly removing galvanic distortion from the magnetotelluric impedance tensor: application to Abitibi and Kapuskasing data (Canada). *Geophys. J. Internat.* 108, 917–929.
- Chave, A.D., Jones, A.G., 1997. Electric and magnetic field distortion decomposition of BC87 data. *J. Geomagn. Geoelectr.* 49, 767–789.
- Chave, A.D., Smith, J.T., 1994. On electric and magnetic galvanic distortion tensor decompositions. *J. Geophys. Res.* 99, 4669–4682.
- Cook, F.A., Erdmer, P., 2005. An 1800 km cross section of the lithosphere through the northwestern North American plate: lessons from 4.0 billion years of Earth's history. *Can. J. Earth Sci.* 42, 1295–1311.
- Cook, F.A., Jones, A.G., 1995. Seismic reflectivity and electrical conductivity: a case of Holmes' curious dog? *Geology* 23, 141–144.
- Davis, W.J., Jones, A.G., Bleeker, W., Grütter, H., 2003. Lithospheric development in the Slave Craton: a linked crustal and mantle perspective. *Lithos* 71, 575–589.
- Debayle, E., Kennett, B.L.N., 2000a. Anisotropy in the Australasian upper mantle from Love and Rayleigh waveform inversion. *Earth Planet. Sci. Lett.* 184, 339–351.
- Debayle, E., Kennett, B.L.N., 2000b. The Australian continental upper mantle: structure and deformation inferred from surface waves. *J. Geophys. Res.* 105, 25, 423–25, 450.
- Du Frane, W.L., Roberts, J.J., Toffelmier, D.A., Tyburczy, J.A., 2005. Anisotropy of electrical conductivity in dry olivine. *Geophys. Res. Lett.* 32, L24315, doi:10.1029/2006GL023879.
- Eaton, D.W., Hope, J., 2003. Structure of the crust and upper mantle of the Great Slave Lake shear zone, northwestern Canada, from teleseismic analysis and gravity modelling. *Can. J. Earth Sci.* 40, 1203–1218.
- Eaton, D.W., Jones, A.G., Ferguson, I.J., 2004. Lithospheric anisotropy structure inferred from collocated teleseismic and magnetotelluric observations: Great Slave Lake shear zone, northern Canada. *Geophys. Res. Lett.* 31, L19614, doi:10.1029/2004GL020939.
- Everett, M.E., 2005. What do electromagnetic induction responses measure? *Leading Edge* 24, 154–157.
- Ferguson, I.J., Edwards, R.N., 1994. Electromagnetic mode conversion by surface-conductivity anomalies: applications for conductivity soundings. *Geophys. J. Int.* 117, 48–68.
- Gatzemeier, A., Moorkamp, M., 2005. 3D modelling of electrical anisotropy from electromagnetic array data: hypothesis testing for different upper mantle conduction mechanisms. *Phys. Earth, Planet. Int.* 149, 225–242.
- Gómez-Trevino, E., 1987. A simple sensitivity analysis of time-domain and frequency-domain electromagnetic measurements. *Geophysics* 52, 1418–1423.
- Groom, R.W., Bailey, R.C., 1989. Some effects of multiple lateral inhomogeneities in magnetotellurics. *Geophys. Prospect.* 37, 697–712.
- Hamilton, M.P., Jones, A.G., Evans, R.L., Evans, S., Fourie, S., Garcia, X., Mountford, A., Spratt J.E., The SAMTEX Team, 2006. Anisotropy structure of the lithosphere derived from magnetotelluric and seismic shear-wave splitting analyses in southern Africa. *Phys. Earth Planet. Inter.*, submitted for publication.
- Heintz, M., Kennett, B.L.N., 2005. Continental scale shear wave splitting analysis: Investigation of seismic anisotropy underneath the Australian continent. *Earth Planet. Sci. Lett.* 236, 106–119.
- Hoffman, P., 1988. United plates of America, the birth of a craton: early Proterozoic assembly and growth of Proto-Laurentia. *Ann. Rev. Earth Planet. Sci.* 16, 543–603.
- Ji, S., Rondenay, S., Mareschal, M., Senechal, G., 1996. Obliquity between seismic and electrical anisotropies as a potential indicator of movement sense for ductile mantle shear zones. *Geology* 24, 1033–1036.
- Jones, A.G., 1983a. The problem of “current channelling”: a critical review. *Geophys. Surv.* 6, 79–122.
- Jones, A.G., 1983b. On the equivalence of the “Niblett” and “Bostick” transformations in the magnetotelluric method. *J. Geophys.* 53, 72–73 (reprinted in Vozoff (1986)).
- Jones, A.G., 1993a. Electromagnetic images of modern and ancient subduction zones. *Tectonophysics* 219, 29–45.
- Jones, A.G., 1993b. The COPROD2 dataset: tectonic setting, recorded MT data and comparison of models. *J. Geomagn. Geoelectr.* 45, 933–955.
- Jones, A.G., 1998. Waves of the future: superior inferences from collocated seismic and electromagnetic experiments. *Tectonophysics* 286, 273–298.
- Jones, A.G., 1999. Imaging the continental upper mantle using electromagnetic methods. *Lithos* 48, 57–80.
- Jones, A.G., Craven, J.A., 1990. The North American Central Plains conductivity anomaly and its correlation with gravity, magnetics, seismic, and heat flow data in the Province of Saskatchewan. *Phys. Earth Planet. Inter.* 60, 169–194.
- Jones, A.G., Craven, J.A., McNeice, G.A., Ferguson, I.J., Boyce, T., Farquharson, C., Ellis, R.G., 1993. The North American Central Plains conductivity anomaly within the Trans-Hudson orogen in northern Saskatchewan. *Geology* 21, 1027–1030.
- Jones, A.G., Ferguson, I.J., Chave, A.D., Evans, R.L., McNeice, G.W., 2001a. The electric lithosphere of the Slave craton. *Geology* 29, 423–426.
- Jones, A.G., Katsube, J., Schwann, P., 1997. The longest conductivity anomaly in the world explained: sulphides in fold hinges causing very high electrical anisotropy. *J. Geomagn. Geoelectr.* 49, 1619–1629.
- Jones, A.G., Ledo, J., Ferguson, I.J., Farquharson, C., Garcia, X., Grant, N., McNeice, G.W., Roberts, B., Spratt, J., Wennberg, G., Wolyne, L., Wu, X., 2005a. The electrical resistivity structure of Archean to Tertiary lithosphere along 3200 km of SNORCLE profiles, northwestern Canada. *Can. J. Earth Sci.* 42, 1257–1275.
- Jones, A.G., Ledo, J., Ferguson, I.J., 2005b. Electromagnetic images of the Trans-Hudson orogen: The North American Central Plains anomaly revealed. *Can. J. Earth Sci.* 42, 457–478.
- Jones, A.G., Lezaeta, P., Ferguson, I.J., Chave, A.D., Evans, R.L., Garcia, X., Spratt, J., 2003. The electrical structure of the Slave craton. *Lithos* 71, 505–527.
- Jones, A.G., Snyder, D., Spratt, J., 2001b. Magnetotelluric and Teleseismic experiments as Part of the Walmsley Lake project: experimental designs and preliminary results. *Geol. Surv. Can. Curr. Res.*, p. C6.
- Jones, A.G., Snyder, D., Hanmer, S., Asudeh, I., White, D., Eaton, D., Clarke, G., 2002. Magnetotelluric and teleseismic study across the Snowbird Tectonic Zone, Canadian Shield: a Neoproterozoic mantle suture? *Geophys. Res. Lett.* 29 (17), doi:10.1029/2002GL015359, 10-1-10-4.

- Kellett, R.L., Mareschal, M., Kurtz, R.D., 1992. A model of lower crustal electrical anisotropy for the Pontiac Subprovince of the Canadian Shield. *Geophys. J. Int.* 111, 141–150.
- Kohlstedt, D., Mackwell, S., 1998. Diffusion of hydrogen and intrinsic point defects in olivine. *Z. Phys. Chem.* 207, 147–162.
- Korja, T., Engels, M., Lahti, I., Kobzova, V., Ladanivskyy, B., The BEAR Working Group, 2002. Is lithosphere anisotropic in the central Fennoscandian shield? In: *Contrib. Paper, EM Induction Workshop, Santa Fe, June*.
- Korja, T., The BEAR Working Group, 2003. Upper mantle conductivity in Fennoscandia as imaged by the BEAR array. *Contrib. paper, EGU, Nice*.
- Kurtz, R.D., Craven, J.A., Niblett, E.R., Stevens, R.A., 1993. The conductivity of the crust and mantle beneath the Kapuskasing Uplift: electrical anisotropy in the upper mantle. *Geophys. J. Int.* 113, 483–498.
- Lahti, I., Korja, T., Kaikkonen, P., Vaittinen, K., BEAR Working Group, 2005. Decomposition analysis of the BEAR magnetotelluric data: implications for the upper mantle conductivity in the Fennoscandian Shield. *Geophys. J. Int.* 165, 900–914.
- Madden, T.R., 1976. Random networks and mixing laws. *Geophysics* 41, 1104–1125.
- Madden, T.R., 1983. Microcrack connectivity in rocks: a renormalization group approach to the critical phenomena of conduction and failure in crystalline rocks. *J. Geophys. Res.* 88, 585–592.
- Mareschal, M., Kellett, R.L., Kurtz, R.D., Ludden, J.N., Bailey, R.C., 1995. Archean cratonic roots, mantle shear zones and deep electrical anisotropy. *Nature* 373, 134–137.
- McNeice, G., Jones, A.G., 2001. Multisite, multifrequency tensor decomposition of magnetotelluric data. *Geophysics* 66, 158–173.
- Narod, B.B., Bennest, J.R., 1990. Ring-core fluxgate magnetometers for use as observatory variometers. *Phys. Earth, Planet. Inter.* 59, 23–28.
- Niblett, E.R., Sayn-Wittgenstein, C., 1960. Variation of the electrical conductivity with depth by the magnetotelluric method. *Geophysics* 25, 998–1008.
- Oldenburg, D.W., 1979. One-dimensional inversion of natural source magnetotelluric observations. *Geophysics* 44, 1218–1244.
- Padilha, A.L., Vitorello, I., Pádua, M.B., Bologna, M.S., 2006. Lithospheric and sublithospheric anisotropy beneath central-southeastern Brazil constrained by long period magnetotelluric data. *Phys. Earth Planet. Inter.*, this issue, submitted for publication.
- Pek, J., Santos, F.A.M., 2002. Magnetotelluric impedances and parametric sensitivities for 1-D anisotropic layered media. *Comp. Geosci.* 28, 939–950.
- Pek, J., Verner, T., 1997. Finite difference modelling of magnetotelluric fields in 2-D anisotropic media. *Geophys. J. Internat.* 128, 505–521.
- Silver, P.G., 1996. Seismic anisotropy beneath the continents: probing the depths of geology. *Ann. Rev. Earth Sci.* 24, 385–432.
- Silver, P.G., Chan, W.W., 1988. Implications for continental structure and evolution from seismic anisotropy. *Nature* 335, 34–39.
- Silver, P.G., Chan, W.W., 1991. Shear-wave splitting and subcontinental mantle deformation. *J. Geophys. Res.* 96, 16, 429–16, 454.
- Simons, F.J., van der Hilst, R.D., 2003. Seismic and mechanical anisotropy and the past and present deformation of the Australian lithosphere. *Earth, Planet. Sci. Lett.* 211, 271–286.
- Simpson, F., 2001. Resistance to mantle flow inferred from the electromagnetic strike of the Australian upper mantle. *Nature* 412, 632–634.
- Simpson, F., 2002. Intensity and direction of lattice-preferred orientation of olivine: are electrical and seismic anisotropies of the Australian mantle reconcilable? *Earth Planet. Sci. Lett.* 203, 535–547.
- Simpson, F., Tommasi, A., 2005. Hydrogen diffusivity and electrical anisotropy of a peridotite mantle. *Geophys. J. Int.* 160, 1092–1102.
- Smith, J.T., 1995. Understanding telluric distortion matrices. *Geophys. J. Internat.* 122, 219–226.
- Smith, J.T., 1997. Estimating galvanic-distortion magnetic fields in magnetotellurics. *Geophys. J. Int.* 130, 65–72.
- Snyder, D.B., Bostock, M.G., Lockhart, G.D., 2003. Two anisotropic layers in the Slave craton. *Lithos* 71, 529–539.
- Snyder, D.B., Rondenay, S., Bostock, M.G., Lockhart, G.D., 2004. Mapping the mantle lithosphere for diamond potential using teleseismic methods. *Lithos* 77, 859–872.
- Stauffer, M.R., 1984. Manikewan: an Early Proterozoic ocean in central Canada, its igneous history and orogenic closure. *Precam. Res.* 25, 257–281.
- Tommasi, A., Tikoff, B., Vauchez, A., 1999. Upper mantle tectonics: three-dimensional deformation, olivine crystallographic fabrics and seismic properties. *Earth Planet. Sci. Lett.* 168, 173–186.
- Vinnik, L.P., Kosarev, G.L., Makeyeva, L.I., 1984. Anisotropy in the lithosphere from the observations of SKS and SKKS. *Dokl. Acad. Nauk. SSSR* 278, 1335–1339.
- Vinnik, L.P., Makeyeva, L.I., Milev, A., Usenko, A.Y., 1992. Global patterns of azimuthal anisotropy and deformations in the continental mantle. *Geophys. J. Internat.* 111, 433–447.
- Wannamaker, P.E., 2005. Anisotropy versus heterogeneity in Continental solid Earth electromagnetic studies: fundamental response characteristics and implications for physicochemical state. *Surv. Geophys.* 26, 733–765.
- Wu, X., Ferguson, I.J., Jones, A.G., 2002. Magnetotelluric response and geoelectric structure of the Great Slave Lake shear zone. *Earth, Planet. Sci. Lett.* 196, 35–50.
- Zhang, P., Roberts, R.G., Pedersen, L.B., 1987. Magnetotelluric strike rules. *Geophysics* 52, 267–278.

Further reading

- Vozoff, K. (Ed.), 1986. *Magnetotelluric Methods*. Soc. Ex pl. Geophys. Reprint Ser. No. 5, Tulsa, OK, ISBN 0-931830-36-2.